

## Research Article

# Efficient Control Channel Resource Allocation for VoIP in OFDMA-Based Packet Radio Networks

**Yong Fan and Mikko Valkama**

*Department of Communications Engineering, Tampere University of Technology, Tampere 33720, Finland*

Correspondence should be addressed to Yong Fan, yong.fan@tut.fi

Received 15 November 2010; Accepted 28 February 2011

Academic Editor: Boris Bellalta

Copyright © 2011 Y. Fan and M. Valkama. This is an open access article distributed under the Creative Commons Attribution License, which permits unrestricted use, distribution, and reproduction in any medium, provided the original work is properly cited.

We propose an efficient control channel resource allocation approach to enhance the performance of voice-over-IP (VoIP) in orthogonal frequency division multiple access- (OFDMA-) based next generation mobile communication systems. As the long-term evolution (LTE) of universal terrestrial radio access network (UTRAN), evolved UTRAN (E-UTRAN) is the first OFDMA-based packet radio network and thus selected in this paper as an application example. Our proposed physical downlink control channel (PDCCH) resource allocation approach for E-UTRAN is composed of bidirectional power control, inner loop link adaptation (ILLA), and outer loop link adaptation (OLLA) algorithms. Its effectiveness is validated through large-scale radio system level simulations, and simulation results confirm that VoIP capacity with dynamic scheduling can be further enhanced with this PDCCH resource allocation approach. Moreover, the VoIP performance requirements for international mobile telecommunications-advanced (IMT-Advanced) radio interface technologies can be met with dynamic scheduling together with proposed PDCCH resource allocation. Besides E-UTRAN, this approach can be introduced to other OFDMA-based mobile communication systems for VoIP performance enhancement as well.

## 1. Introduction

Mobile communication systems are gradually transforming from the systems mainly oriented to voice service to ones that can handle more high data rate services. Although data services are getting more momentum during this transformation, voice service still remains as the main source of revenue for mobile network operators [1]. For savings in capital expenditures and operating expenses, there is also a clear trend that all services are gradually being converged into packet switched (PS) domain. Related work [2–4] on supporting voice service through VoIP protocol in Third Generation cellular network, for example, high speed packet access (HSPA), have already been conducted. The future mobile networks will be completely IP-based and traditional circuit switched (CS) domain will not exist any more in them. Therefore, efficient VoIP support is a fundamental requirement for any emerging new systems.

The next generation mobile communication systems, for example, universal terrestrial radio access network (UTRAN) long-term evolution (LTE) and LTE-Advanced, worldwide

interoperability for microwave access (WiMax), and ultra mobile broadband (UMB), all rely on orthogonal frequency division multiple access (OFDMA) as multiple access scheme. Conveying voice service through VoIP protocol in OFDMA-based mobile communication systems inevitably faces challenges caused by inherent VoIP traffic characteristics and stringent quality of service (QoS) criteria. VoIP traffic is low and constant bit-rate traffic, implying small size VoIP packets are transmitted at regular time intervals. The resource allocation for packet transmission is relatively small, thus necessitating multiuser sharing in frequency domain to effectively utilize available wide frequency bandwidth. Moreover, VoIP packets have to be scheduled frequently in order to satisfy the strict packet delay and loss based QoS criteria. In a typical packet radio system, such as evolved UTRAN (E-UTRAN), the transmission of each packet is done with dynamic scheduling by default [5] and evolved NodeB (eNB) needs to signal scheduled user equipment (UE) the resource allocation information through physical downlink control channel (PDCCH) every scheduling period, for example, one transmission time interval (TTI). As a result,

the simultaneous scheduling of multiple users in a frequent manner demands lots of physical layer control signaling resources. The situation on control signaling consumption is further deteriorated by high VoIP capacity demand in PS radio network, which is supposed to accommodate a large amount of voice capacity currently handled in traditional CS mode.

Since the future mobile communication systems also target for high data rate transmission, it is preferable to allocate more radio resources for data transmission, thus leaving few resources for control signaling. Therefore, deploying VoIP in OFDMA-based packet radio systems encounters one unique challenge, that is, to satisfy high VoIP capacity demand with only limited physical layer control signaling resources. In E-UTRAN, PDCCH carries scheduling grants for both downlink and uplink, and its overall design was addressed in [6]. During the E-UTRAN standardization in Third Generation Partnership Project (3GPP), different solutions and schemes [7–11] have already been studied to overcome the limitations of PDCCH resources on VoIP capacity. All these aim at reducing the consumption of PDCCH resources and the possibility of conducting effective PDCCH resource allocation is not considered. The existing UTRAN LTE system level simulation results [9, 12] using simplified PDCCH modeling show that VoIP capacity with dynamic scheduling is limited by available PDCCH resources. The studies [13, 14] using realistic PDCCH modeling further confirm such limiting effect. Compared with delay-tolerant full buffer traffic, the impact of PDCCH limitation on delay-sensitive VoIP traffic is much more severe. While PDCCH limitation causes only marginal loss of cell throughput with full buffer traffic and there is also no evident relationship between cell throughput and the number of users scheduled per TTI [15], VoIP capacity in E-UTRAN is directly proportional to the number of users scheduled simultaneously in each TTI [13, 14]. On the other hand, it also implies great potential to significantly enhance VoIP capacity if effective PDCCH resource allocation is in place. However, the related study is obviously missing in available open literature.

To meet the ambitious performance target for international mobile telecommunication-advanced (IMT-Advanced) candidate radio interface technologies (RITs) [16], LTE is evolving into LTE-Advanced, and VoIP performance also needs to be improved. In the LTE-Advanced self-evaluation inside 3GPP, both dynamic scheduling and semipersistent scheduling are considered. While all existing solutions and schemes, such as dynamic packet bundling [9] and semipersistent scheduling [10, 11], try to reduce consumption of control channel resources, we consider a new paradigm in this paper to overcome limitation of control channel resources and further enhance VoIP performance, that is, to allocate limited control channel resources more effectively so that we can schedule more VoIP users dynamically in each TTI. Our proposed PDCCH resource allocation approach includes bidirectional power control, inner loop link adaptation (ILLA), and outer loop link adaptation (OLLA) algorithms. They are simple yet efficient and can be easily implemented requiring no changes to the existing 3GPP technical specifications.

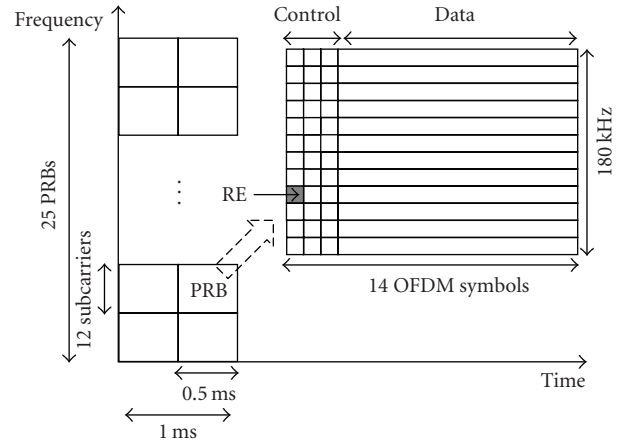


FIGURE 1: Time-frequency resource structure of E-UTRA.

The remainder of this paper is structured as follows. Section 2 gives a brief introduction of evolved universal terrestrial radio access (E-UTRA), the air interface of UTRAN LTE downlink as well as VoIP QoS and capacity criteria. Section 3 presents the design of proposed PDCCH resource allocation approach and related wideband channel quality indicator (CQI) measurement model and dynamic scheduling algorithm. Section 4 describes the overall simulation environment for VoIP on E-UTRA and used VoIP traffic model. The system simulation results in both 3GPP LTE and ITU IMT-Advanced scenarios are examined and analyzed in Section 5 before we draw final conclusions in Section 6.

## 2. VoIP on E-UTRA

**2.1. E-UTRA Overview.** Figure 1 illustrates time-frequency resource structure of E-UTRA [17]. In time domain, the duration of one subframe, also called transmission time interval (TTI) is 1 ms, consisting of 2 equally sized time slots of 0.5 ms. Each time slot accommodates 6 or 7 OFDM symbols, depending on whether a short or extended cyclic prefix is applied. In each TTI, the first 1 to 3 OFDM symbols can be allocated for control signaling and the remaining OFDM symbols are used for data transmission. In this study, we assume that each TTI contains 14 OFDM symbols and the first 3 OFDM symbols are all reserved for control channels. In frequency domain, the minimum resource unit allocated for user data transmission is physical resource block (PRB), each containing 12 adjacent subcarriers with sub-carrier spacing of 15 kHz. In this study, we use a configuration of 5 MHz spectrum allocation with 25 PRBs. In time-frequency resource grid, resource element (RE) is the smallest time and frequency resource, spanning over 1 OFDM symbol in time domain and 1 sub-carrier in frequency domain. The minimum resource unit allocated to user for control signaling is control channel element (CCE) containing 36 REs which are distributed over time duration of 3 OFDM symbols and the whole frequency bandwidth. In 5 MHz spectrum allocation, the total number of CCEs is 20 which

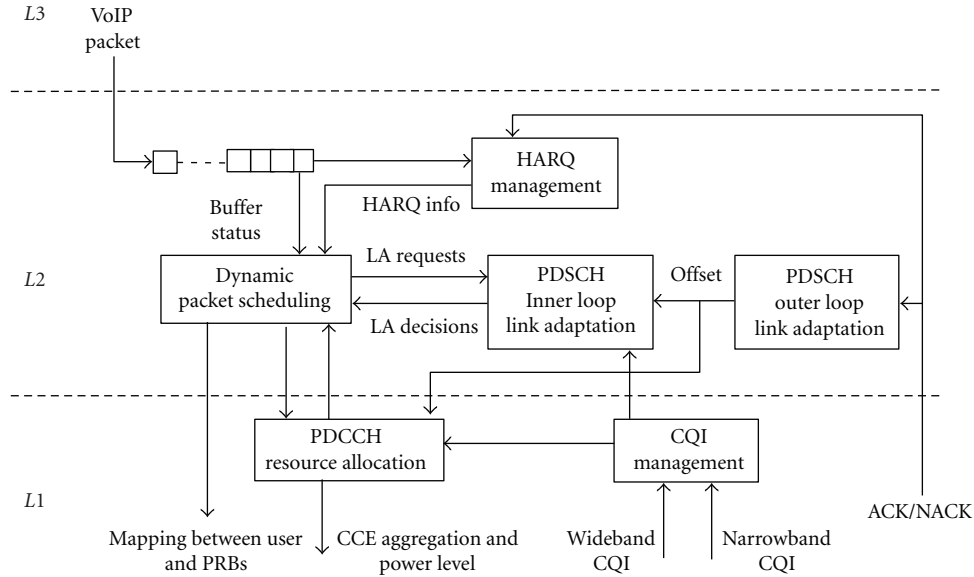


FIGURE 2: Main RRM functionalities and their interactions in eNB.

are assumed to be equally divided between downlink and uplink.

**2.2. VoIP QoS and Capacity Criteria.** For voice service, the one way end-to-end delay should be below 250 ms to guarantee relatively good voice quality rating [18]. The packet delay includes delay in evolved packet core (EPC) and E-UTRAN. Since the focus of this study is on E-UTRAN part, we deduct packet processing delay and propagation delay of approximately 100 ms in EPC, the delay budget left for E-UTRAN is around 150 ms. We further assume that both end-users are E-UTRAN users, the tolerable delay for medium access control (MAC) queuing and scheduling as well as physical (PHY) transmission should be strictly within 80 ms. To further improve voice quality and better account for variability in network, 3GPP uses 50 ms air interface delay bound (one-way delay from eNB to UE) in LTE system performance evaluation [19]. According to satisfied user criterion (SUC) also specified in [19], a user is regarded as satisfied if 98% of packets for the user are received successfully within 50 ms air interface delay bound when monitored over the duration of the whole voice call. The VoIP system capacity is further defined as the number of users per cell when more than 95% of the users in the cell are satisfied.

### 3. PDCCH Resource Allocation and Related RRM Algorithms

Figure 2 illustrates the main radio resource management (RRM) entities located in eNB as well as interactions between them. Based on the buffer status, hybrid ARQ (HARQ) info, and used scheduling metric, dynamic packet scheduler generates a schedulable user list and then feeds

it to PDCCH resource allocation unit for resource availability check. PDCCH resource allocation unit sequentially allocates control resources to user in the same order as that in the schedulable user list. Depending on the feedback from PDCCH resource allocation unit, dynamic scheduler selects users to be scheduled according to PDCCH resource constraints and allocate PRBs for user data transmission. Dynamic scheduler also consults physical downlink shared channel (PDSCH) inner loop link adaptation to determine the number of PRBs allocated to each user and MCS for each PRB. In this section, we will introduce the proposed PHY layer PDCCH resource allocation and closely related algorithms, such as CQI management and MAC layer dynamic packet scheduling.

**3.1. PDCCH Overview.** PDCCH carries downlink scheduling assignments and uplink scheduling grants. The information fields in the scheduling assignments and scheduling grants include resource allocation information, transport format information, and HARQ information. Since there is no HARQ mechanism in PDCCH and the failure of PDCCH transmission will directly lead to failure of subsequent PDSCH transmission, the BLER target is set to 1% for the purpose of reliable PDCCH transmission. The MCS for transmission of PDCCH payload is QPSK modulation with four different effective coding rates of 2/3, 1/3, 1/6, and 1/12, corresponding to aggregation level of 1, 2, 4, 8 CCEs, respectively. A user in favorable radio channel conditions may require just 1 CCE with QPSK 2/3. Adaptive coding can be used to aggregate 2, 4, or even 8 CCEs with lower effective coding rate, thus improving the PDCCH coverage for users in worse radio channel conditions.

**3.2. CQI Measurement Model.** We determine the CCE aggregation level for each UE based on wideband CQI value as it

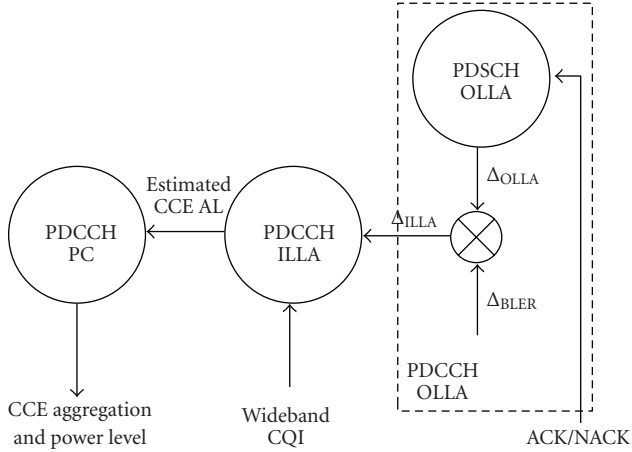


FIGURE 3: PDCCH resource allocation: power control and link adaptation.

reflects the average channel condition of UE. Wideband CQI is produced by taking the average of all ideal signal to interference noise ratio (SINR) values measured on each narrow subband across the whole frequency bandwidth. Therefore, the accuracy of wideband CQI modeling is greatly dependent on that of narrowband CQI modeling. The narrowband CQI modeling follows the framework presented in [20]. Each UE periodically measures SINR on time duration  $\Delta t$  and subband bandwidth  $\Delta f = N \cdot 180$  kHz, where  $N$  is the consecutive number of PRBs within each measurement subband. To facilitate opportunistic scheduling in both time domain and frequency domain,  $\Delta t$  and  $\Delta f$  should be set to sufficiently small values so that frequency selectivity and time-variant behavior of radio channel can be well captured. Here,  $\Delta t = 2$  ms and  $\Delta f = 360$  kHz are used. The measured narrowband SINR is subject to an additive error due to limited number of pilot symbols within each subband. As the averaging value of narrowband SINRs, wideband SINR  $\text{SINR}_{\text{WB}}$  is also subject to error, which is modeled as a zero-mean Gaussian random variable with standard deviation  $\sigma_{\text{WB}} = 0.2$  dB. The measured realistic wideband SINR is then quantized to discrete CQI values ready for reporting. In UTRAN LTE downlink, the dynamic range of modulation and coding scheme (MCS) from quaternary phase shift keying (QPSK) with excessive coding to 64-quadrature amplitude modulation (64-QAM) with marginal coding is approximately 25 dB, which can be covered in 5 bits with quantization step size of  $\Delta_{\text{cqi}} = 1$  dB. The generated wideband CQI  $\text{CQI}_{\text{WB}}$  is expressed as

$$\text{CQI}_{\text{WB}} = \Delta_{\text{cqi}} \times \text{round} \left( \frac{\text{SINR}_{\text{WB}} + \sigma_{\text{WB}}}{\Delta_{\text{cqi}}} \right), \quad (1)$$

where  $\text{round}(\cdot)$  is the operation of rounding to the nearest integer. Finally, the quantized wideband CQIs are reported to eNB with specified reporting schemes subject to certain feedback delay.

**3.3. PDCCH Power Control and ILLA Algorithms.** As seen in Figure 3, PDCCH resource allocation is composed of power

control algorithm and link adaptation (LA) algorithm, which is further divided into ILLA and OLLA. PDCCH ILLA is responsible for estimating CCE aggregation level based on user's wideband CQI and adjustment offset from PDCCH OLLA algorithm. PDCCH power control is the key element in resource allocation. It determines the finally selected CCE aggregation and power level as well as balances allocation of power and CCE. Since power control and ILLA work closely with each other, we introduce them together here.

Previous study [15] on PDCCH resource allocation for full buffer traffic proposed a power boost algorithm. It artificially lowers CCE aggregation level by adding an initial power offset on user's wideband CQI before determining the required number of CCE. However, using high power offset will quickly run out of power while on the contrary CCE will easily be depleted if low power offset is applied. Therefore, it is hardly optimal in both power domain and CCE domain. In this study, we come up with a bidirectional power control algorithm to effectively balance the allocation of PDCCH power and CCEs, thus maximizing the number of dynamically scheduled users per TTI. The proposed PDCCH resource allocation can be divided into three steps and functions as follows.

*Step 1.* Estimate CCE aggregation level: the estimated CCE AL  $\tilde{N}_{\text{CCE}}$  is determined by choosing the minimum required number of CCEs satisfying equation  $\text{SINR}_{\text{WB}} \geq \text{SINR}_{\text{required}, \tilde{N}_{\text{CCE}}}$ , where  $\text{SINR}_{\text{WB}}$  is user's wideband CQI taking into account measurement error and quantization effect as well as feedback delay,  $\text{SINR}_{\text{required}, \tilde{N}_{\text{CCE}}}$  is the required SINR to reach the PDCCH target BLER of 1% with  $\tilde{N}_{\text{CCE}}$ .

*Step 2.* Determine the actual CCE aggregation level and transmission power: without power control, the actual CCE AL would simply be  $N_{\text{CCE}} = \tilde{N}_{\text{CCE}}$ . The normal transmission power per sub-carrier would be  $\bar{P}_{\text{sc}} = P_{\text{eNB}}/N_{\text{sc}}$ , where  $P_{\text{eNB}}$  is the total eNB transmission power in mW, and  $N_{\text{sc}}$  is the total number of subcarriers within the system bandwidth. Then, the PDCCH transmission power for user would be

$$\left( P_{\text{PDCCH}} = \bar{P}_{\text{sc}} \cdot \frac{N_{\text{RE}}}{N_{\text{sym}}} = \bar{P}_{\text{sc}} \cdot \frac{N_{\text{CCE}} \cdot k}{N_{\text{sym}}} \right), \quad (2)$$

where  $N_{\text{RE}}$  is the required number of REs for user,  $N_{\text{sym}}$  is the number of OFDM symbols reserved for PDCCH per TTI, and  $k$  is the size of one CCE in terms of the number of REs.

With proposed power control algorithm, an individual power scaling factor  $P_{\text{SF}}$  for user is applied on the top of normal sub-carrier transmission power  $\bar{P}_{\text{sc}}$  to determine actual sub-carrier transmission power. The PDCCH transmission power for user

$$P_{\text{PDCCH}} = 10^{P_{\text{SF}}/10} \cdot \bar{P}_{\text{sc}} \cdot \frac{N_{\text{CCE}} \cdot k}{N_{\text{sym}}}. \quad (3)$$

The algorithm to determine this user-specific power scaling factor  $P_{\text{SF}}$  and actual CCE AL  $N_{\text{CCE}}$  is illustrated using pseudocode below. For user consuming only one CCE,

power reduction is conducted. For user consuming more than 1 CCE, either power reduction or boost is conducted depending on the additional amount of power needed to reach next lower CCE AL.

```

if  $\tilde{N}_{\text{CCE}} = 1$  then
     $P_{\text{SF}} = \max(\text{SINR}_{\text{required}}, \tilde{N}_{\text{CCE}} - \text{SINR}_{\text{WB}}, P_{\text{maxdecrease}})$ ;
     $N_{\text{CCE}} = 1$ ;
else if  $\tilde{N}_{\text{CCE}} = 2, 4, 8$  then
     $P_{\text{SF}} = \text{SINR}_{\text{required}}, \tilde{N}_{\text{CCE}}/2 - \text{SINR}_{\text{WB}}$ ;
    if  $P_{\text{SF}} < P_{\text{maxincrease}}$  then
         $N_{\text{CCE}} = \tilde{N}_{\text{CCE}}/2$ ;
         $P_{\text{SF}} = \text{SINR}_{\text{required}}, \tilde{N}_{\text{CCE}}/2 - \text{SINR}_{\text{WB}}$ ;
    else if  $P_{\text{SF}} > P_{\text{maxincrease}}$  then
         $N_{\text{CCE}} = \tilde{N}_{\text{CCE}}$ ;
         $P_{\text{SF}} = \text{SINR}_{\text{required}}, \tilde{N}_{\text{CCE}} - \text{SINR}_{\text{WB}}$ ;
    end if
end if
    
```

(4)

$P_{\text{maxdecrease}}$  is the maximum amount of power allowed to be reduced for each user and  $P_{\text{maxincrease}}$  is the maximum amount of power allowed to be boosted for each user. Their values are set within the dynamics of eNB power amplifier and the absolute value of  $P_{\text{maxdecrease}}$  is larger than that of  $P_{\text{maxincrease}}$  to enable conservative power boost and aggressive power reduction.

*Step 3.* Balance allocation of CCE and power: depending on whether there is still CCE or power left, the algorithm enters into the final step to balance CCE and power allocation. If there is power left, the algorithm will try to boost the power of user who originally cannot reach  $\tilde{N}_{\text{CCE}}/2$  CCE in Step 2 due to the limitation from  $P_{\text{maxincrease}}$ . If there is CCE left, the algorithm will try to reduce the power of user who is originally boosted to  $\tilde{N}_{\text{CCE}}/2$  CCE in Step 2.

*3.4. PDCCH OLLA Algorithm.* Since CQI feedback from UE is subject to measurement error and reporting delay as well as other imperfections, OLLA algorithm is then employed to control the experienced average block error rate (BLER) for PDCCH transmissions. A classic OLLA algorithm follows the same principle of outer loop power control algorithm [21], and it relies on the success or failure of past transmissions to determine a compensation offset to ILLA algorithm. If an acknowledgement (ACK) is received for the first transmission, compensation offset factor  $\Delta_{\text{OLLA}}$  is decreased by  $\Delta_{\text{down}}$ . On the contrary, if a negative acknowledgement (NACK) is received for the first

transmission, compensation offset factor  $\Delta_{\text{OLLA}}$  is increased by  $\Delta_{\text{up}}$ . The ratio of  $\Delta_{\text{up}}$  to  $\Delta_{\text{down}}$  determines the average BLER to which OLLA converges, as expressed in formula (5). There is one independent OLLA algorithm maintained for each user,

$$\text{BLER} = \frac{1}{1 + (\Delta_{\text{up}}/\Delta_{\text{down}})}. \quad (5)$$

Unlike PDSCH which can directly apply such type of OLLA, PDCCH cannot do so due to the lack of acknowledgment mechanism in PDCCH. Therefore, we rely on PDSCH OLLA to indirectly control the average BLER for PDCCH. The compensation offset factor  $\Delta_{\text{OLLA}}$  generated from PDSCH OLLA is then scaled by a factor  $\Delta_{\text{BLER}}$  to compensate the difference between BLER targets for PDSCH and PDCCH transmission. After that, the sum of these two factors is fed into PDCCH ILLA algorithm as  $\Delta_{\text{ILLA}}$  for CCE aggregation level estimation.

*3.5. Dynamic Scheduling Algorithm.* A VoIP optimized dynamic scheduling algorithm [9] is used together with proposed PDCCH resource allocation method. The algorithm is separated into two parts: selecting users and assigning PRBs to users. In the user selection, we introduce a two-step scheduling candidate set (SCS) approach to efficiently control the interuser fairness as well as directly address the specific requirements for VoIP traffic scheduling.

For interuser fairness control, all the schedulable users on the basis of eNB buffer status are first sorted according to a relative wideband CQI metric and then organized into primary SCS. Instead of using traditional proportional fair metric based on user throughput, we come up with this new relative wideband CQI metric for interuser fairness control. The relative wideband CQI is defined as  $\text{CQI}_{\text{inst}}(t)/\text{CQI}_{\text{avg}}(t)$ , where  $\text{CQI}_{\text{inst}}(t)$  is instantaneous wideband CQI and  $\text{CQI}_{\text{avg}}(t)$  represents the average wideband CQI in the past.  $\text{CQI}_{\text{avg}}(t)$  is calculated with traditional recursive method [22] by replacing user throughput with CQI value. Relative wideband CQI reflects user's instantaneous channel condition relative to the average and therefore indicates a favorable time instant for scheduling.

To address specific requirements for VoIP traffic scheduling, we further apply the following criteria of user classification on the primary SCS and users are then categorized into 3 groups in the secondary SCS for final user selection:

- (1) users with pending retransmission,
- (2) users whose delay of the oldest unsent packet in the eNB buffer is close to given threshold, and
- (3) remaining users other than the above two groups.

In PDSCH, there is no power control mechanism and each PRB is assigned with the same power level. The number of PRB allocated to each user is determined by adaptive approach based on user's channel condition. As for assigning PRBs to selected users, we give priority to first transmission users in choosing PRBs with relatively favorable channel quality and grant the retransmission users the priority to

reserve the same amount of PRBs as in the original transmissions. By doing so, a high successful rate of first transmission can be achieved and then packet transmission delay over the air interface is reduced. Besides, retransmission users can anyway benefit from HARQ combining gain for correct reception, although they are given less freedom to choose suitable PRBs.

#### 4. System Level Simulation Setup

**4.1. Overall Simulation Environment.** We have developed a quasistatic system level simulator to investigate the effect of proposed PDCCH resource allocation on VoIP capacity enhancement. This simulation tool has been used extensively in generating various UTRAN LTE and LTE-Advanced performance evaluation results for 3GPP contributions and conforms to the guidelines specified in [19]. In the simulations, the related radio resource management algorithms shown in Figure 1 are all explicitly modeled. To reduce simulation time and facilitate easy comparison with existing results of VoIP on E-UTRA [9, 10, 12, 14], we consider 5 MHz system bandwidth configuration in all the deployment scenarios. The physical layer parameter settings are based on [17] and the physical layer performance of single radio link is obtained from separate link level simulations and fed to system level simulations through exponential effective SINR metric (EESM) [23]. The simulated network layout is a hexagonal grid composed of 19 cell sites with 3 sectors each. At the beginning of each simulation run, 2-Rx maximum ratio combining (MRC) receiver UEs are randomly placed in the simulation area and keep the position unchanged during this simulation run. Thus, distance-dependent path loss and shadow fading are constant while fast fading is updated every TTI according to the selected radio channel model, for example, typical urban (TU) 20 taps channel model for 3GPP LTE scenario. System level simulations are conducted with time resolution of one TTI, and several independent simulation runs are conducted to gather enough statistics. The main simulation assumptions are also summarized in Table 1.

**4.2. VoIP Traffic Model.** VoIP traffic is generated from adaptive multi rate (AMR) voice codec [24], which is widely used in 3GPP performance evaluation. Voice activity of user is modeled using 2-state Markov model recommended in [19]. In the case of using AMR 12.2 codec, voice encoder generates a voice frame of 31 bytes payload every 20 ms during activity periods. During silence periods, a silence descriptor (SID) frame of 5 bytes is sent for comfort noise generation purpose every 160 ms. Voice frame is encapsulated sequentially with network protocols including real-time transport protocol (RTP), user datagram protocol (UDP), and IP. After that, it is further encapsulated with radio protocols including packet data convergence protocol (PDCP), radio link control (RLC), and medium access control (MAC). The combined protocol header of 40 bytes for IPv4 will seriously degrade the air interface efficiency, thus necessitating robust header compression (RoHC). The total 9 bytes protocol overhead of

TABLE 1: Main simulation parameters and values.

| Parameter                  | Value  |
|----------------------------|--|
| Deployment scenario        | 3GPP LTE: Macro Case 1 and 3   |
|                            | ITU IMT-A: indoor hotspot, urban microcell, urban macrocell, and rural macrocell |
| HARQ                       | Asynchronous adaptive with chase combining                                       |
|                            | Num. of stop-and-wait processes: 8   |
|                            | Max. number of retransmissions: 3  |
| CQI                        | Measurement time duration: 2 ms  |
|                            | Measurement subband bandwidth: 360 KHz   |
|                            | Narrowband error standard deviation: 1 dB  |
|                            | Wideband error standard deviation: 0.2 dB  |
|                            | Quantization step: 1 dB  |
| PDSCH                      | Feedback delay: 2 ms   |
|                            | Measurement period: 5 ms   |
|                            | Transmission power: 12 W (Macro scenario)  |
|                            | Num. of data OFDM symbols per TTI: 11  |
|                            | Num. of PRBs: 25   |
|                            | Num. of subcarriers: 300   |
|                            | BLER target: 10%   |
|                            | OLLA step up: 0.5 dB   |
|                            | OLLA step down: 0.05 dB  |
|                            | Max. OLLA step up: 3 dB  |
| Max. OLLA step down: -1 dB |  |
| PDCCH                      | Transmission power: 8 W (Macro scenario)   |
|                            | Num. of control OFDM symbols per TTI: 3  |
|                            | Num. of CCEs (REs): 10 (360)   |
|                            | BLER target: 1%  |
|                            | Max. power increase: +2 dB   |
|                            | Max. power decrease: -4 dB   |

compressed RTP/UDP/IP header [25] and PDCP/RLC/MAC header is added to each voice packet. The most important characteristics of VoIP traffic are summarized in Table 2.

#### 5. Simulation Results Analysis

This section presents simulated system performance of VoIP on E-UTRA in both 3GPP LTE and ITU IMT-A deployment scenarios. The VoIP capacity is evaluated according to SUC criteria described in Section 2.2. All the figures below are plotted with system load corresponding to 95% satisfaction point.

TABLE 2: VoIP traffic characteristics.

| Parameter                          | Value             |
|------------------------------------|-------------------|
| AMR voice codec rate               | 12.2 kbps         |
| Voice call length                  | 60 s              |
| Voice activity factor              | 50%               |
| Mean of active period duration     | 2 s               |
| Mean of silence period duration    | 2 s               |
| Voice/SID packet size              | 40 bytes/15 bytes |
| Voice/SID packet interarrival time | 20 ms/160 ms      |

TABLE 3: 3GPP LTE deployment scenarios.

| Deployment scenario | Macro case 1   | Macro Case 3   |
|---------------------|----------------|----------------|
| Carrier frequency   | 2 GHz          | 2 GHz          |
| Penetration loss    | 20 dB          | 20 dB          |
| UE speed            | 3 km/h         | 3 km/h         |
| Network layout      | Hexagonal grid | Hexagonal grid |
| Intersite distance  | 500 m          | 1732 m         |

5.1. Capacity Enhancement with Proposed PDCCH Resource Allocation. The simulations are conducted for 3GPP Macro Case 1 and Case 3 deployment scenarios, of which the configurations are detailed in Table 3. Case 1 is an interference-limited scenario while Case 3 is an extremely noise-limited scenario in which the intersite distance is over 3 times that of Case 1. Besides enhanced performance with proposed PDCCH power control, baseline performance without PDCCH power control is also simulated for benchmarking purpose. Both without packet bundling and with packet bundling cases are considered. For packet bundling, a maximum of two packets is allowed to be sent together in one TTI to each UE.

5.1.1. VoIP Capacity Gain Analysis. Figures 4 and 5 summarize the achieved VoIP capacity and the relative capacity gain with PDCCH power control over without PDCCH power control. As shown in Figure 4, employing proposed PDCCH power control algorithm provides significant capacity gain over baseline performance without using PDCCH power control. The capacity gain ranges from 31% to 46%, depending on deployment scenario and whether packet bundling is enabled or not.

One observation from Figures 4 and 5 is that power control gain in Case 3 is relatively higher than that in Case 1, either without bundling or with bundling. In Case 3, users experience lower SINR on average due to larger intersite distance and thus consume more PDCCH resources than those in Case 1. Therefore, users in Case 3 benefit more from PDCCH power control.

The effectiveness of this power control algorithm is also validated from Figures 6 and 7. Figure 6 shows the distribution of CCE aggregation level per user, and Figure 7 shows the cumulative distribution function (CDF) of number of users scheduled per TTI, all using statistics collected from simulations in Case 3. As seen in Figure 6, CCE aggregation level of 4, 8 is reduced and aggregation level of 1, 2 is

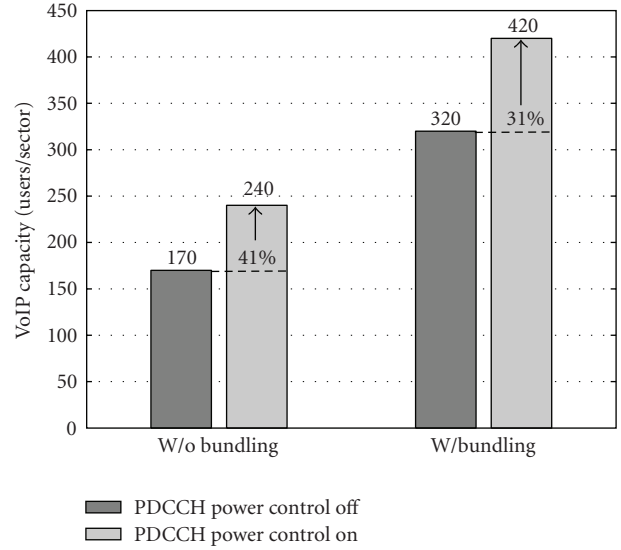


FIGURE 4: VoIP capacity comparison between without PDCCH power control and with PDCCH power control in 5 MHz system bandwidth (Macro Case 1).

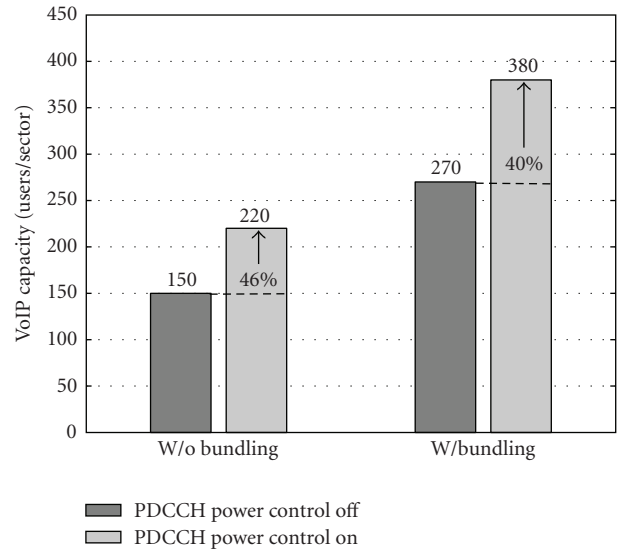


FIGURE 5: VoIP capacity comparison between without PDCCH power control and with PDCCH power control in 5 MHz system bandwidth (Macro Case 3).

increased correspondingly with the aid of PDCCH power control. As a whole, the average aggregation level of user is lowered and the number of users scheduled per TTI is increased, which is also confirmed from Figure 7. As seen in Figure 7, the curve is shifted to the right side with the help from PDCCH power control, indicating the number of users scheduled per TTI is increased on average. In an OFDMA system, the increased number of VoIP users scheduled per TTI directly leads to increased VoIP capacity.

Another observation from Figures 4 and 5 is the capacity gain from packet bundling is not compromised with proposed PDCCH power control. Our PDCCH resource

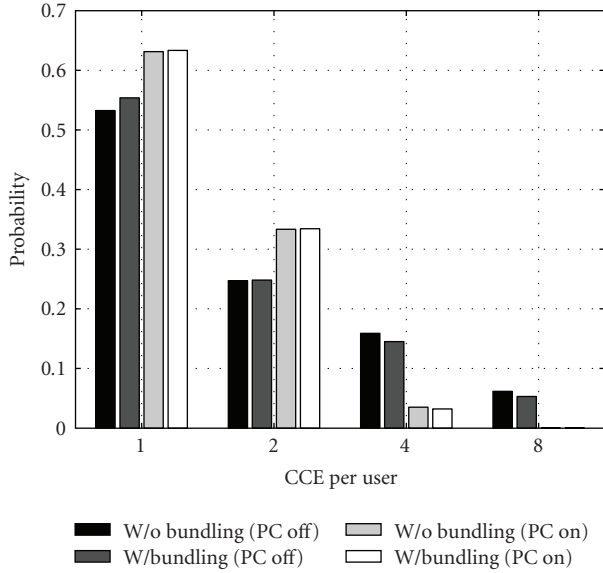


FIGURE 6: Distribution of CCE aggregation level (Macro Case 3).

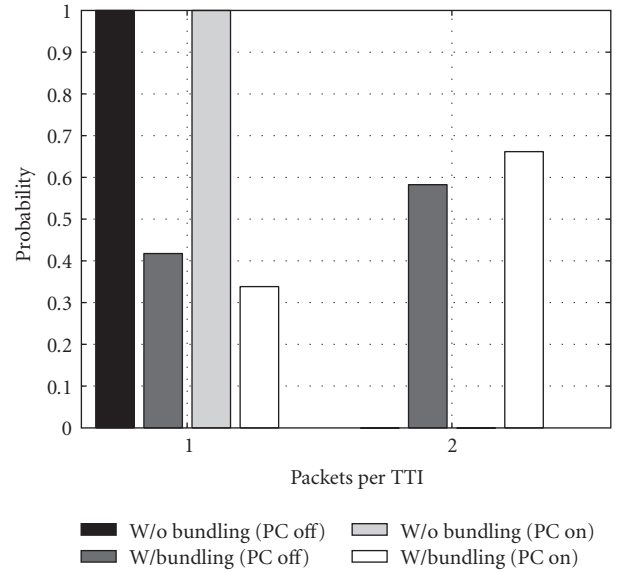


FIGURE 8: Distribution of the number of transmitted packets to each user per TTI (Macro Case 3).

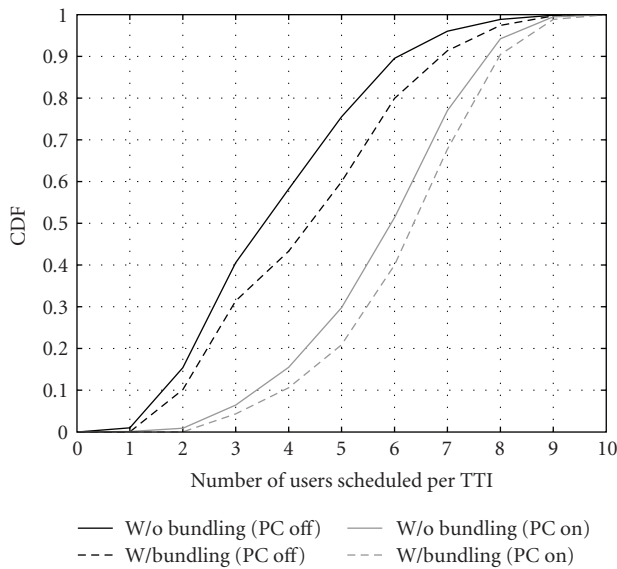


FIGURE 7: CDF of the number of users scheduled per TTI (Macro Case 3).

allocation method strictly follows the calculated scheduling priority in user selection and does not prioritize the users in favorable channel conditions in PDCCH resource allocation. Therefore, users in favorable channel conditions always have enough time to accumulate two packets for bundling, and the packet bundling level can be guaranteed. It is also validated from Figure 8 which shows the distribution of transmitted packets to each user per TTI. As seen in Figure 8, without power control, two-packet transmissions occupy around 60% of total transmissions in Case 3. With power control, the bundling level is even increased a bit.

### 5.1.2. PDCCH and PDSCH Resource Utilization Analysis.

Figure 9 shows the CDF of the amount of PDCCH resources utilized per TTI, in terms of RE and power. Without power control, the transmission power for each CCE is at the same level and PDCCH resource allocation is conducted actually only on one dimension: CCE. Power is allocated in discrete quantities following the number of allocated CCEs. As seen in Figure 9, the shape of CDF of the number of REs used per TTI is exactly the same as that of CDF of the amount of PDCCH power used per TTI. Such kind of plain power allocation obviously leads to the waste of power resources in PDCCH. Therefore, PDCCH power is wasted mostly on users consuming 8, 4, or even 2 CCEs.

With proposed PDCCH power control, the resource allocation is conducted on two dimensions: CCE and power. CCE is still allocated in discrete quantities, but power is instead allocated in continuous quantities, as can be observed from Figure 9. The over-allocated power on user with CCE aggregation level of 8, 4, 2 is used to exchange for reduction of CCE aggregation level to 4, 2, 1. The saved power from users consuming 1 CCE can also be used for this purpose. As a result, not only the total number of CCEs used per TTI can be decreased, but also the assigned power per TTI can be reduced. As also observed from Figure 9, the amount of used power and CCEs with power control is well below that without power control, although the achieved capacity is 40–46% higher. The average utilization rate of CCEs and power is approximately 80%, indicating the efficient balance between CCE and power allocation can also be achieved with this algorithm.

Figure 10 shows the CDF of the number of PRBs scheduled per TTI. Without power control, the average utilization rate of PRBs is only 40% even with the help from packet bundling. More than half of the PDSCH resource can not be efficiently exploited as there are not enough CCEs

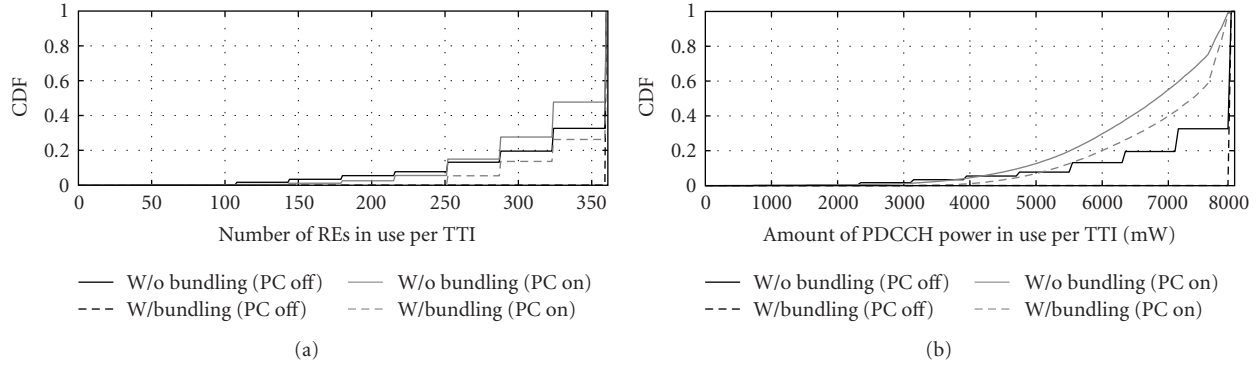


FIGURE 9: CDF of utilization rate of PDCCH CCE and power per TTI (Macro Case 3).

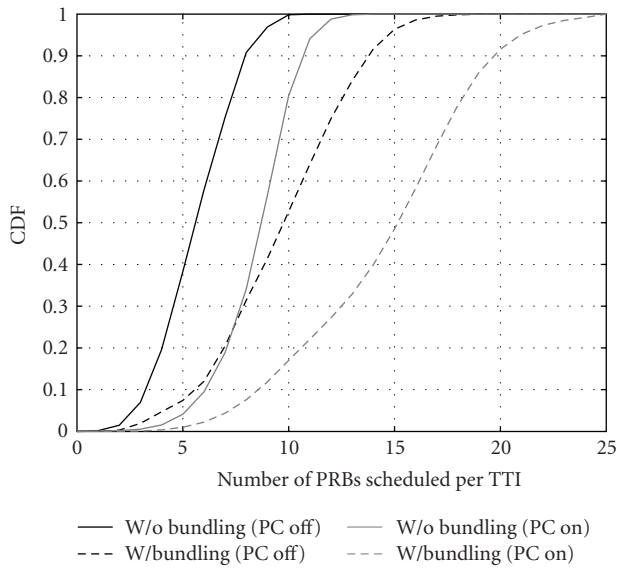


FIGURE 10: CDF of the number of PRBs scheduled per TTI (Macro Case 3).

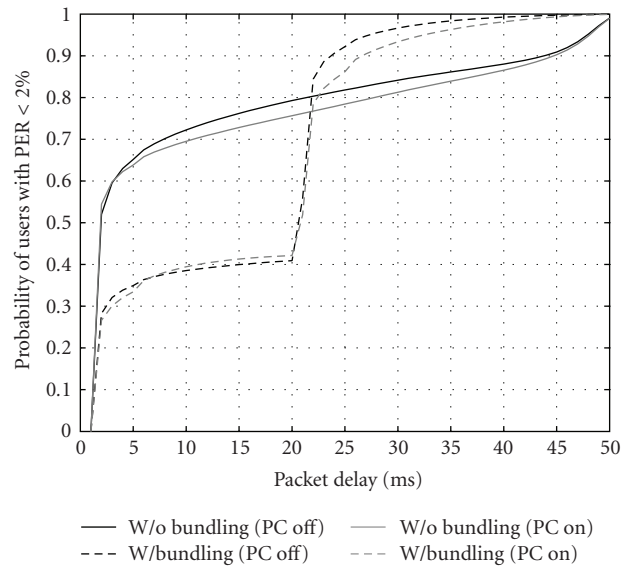


FIGURE 11: CDF of packet delay (Macro Case 3).

to schedule unused PRBs. With proposed power control, the average aggregation level of CCE is lowered and more users can be scheduled per TTI, leading to more efficient exploitation of PDSCH resources. As observed, the average utilization rate increases to 80% with power control. There is still space to increase VoIP capacity with dynamic scheduling by using transmit diversity in eNB and interference rejection combining (IRC) receiver in UE to further increase SINR and reduce the amount of PDCCH resources required by UE.

**5.1.3. VoIP Packet Delay Analysis.** Figure 11 shows the CDF of experienced packet delay for VoIP user. As observed, employing proposed power control does not deteriorate the delay performance. VoIP packet delay is mainly composed of two parts: queuing delay in eNB buffer and transmission delay over the air. With proposed power control, more users can be scheduled per TTI and the queuing delay in eNB buffer is reduced. Although the system load with power control is 46% higher than that without power control,

the curve for without bundling is only slightly shifted to right side, implying minor increase in overall packet delay experienced by user. It is also the same case with bundling.

**5.2. Capacity Evaluation for IMT-Advanced.** IMT-Advanced candidate RITs are required to be applied in a variety of deployment scenarios and support a range of environments. ITU deployment scenarios chosen by 3GPP for LTE-Advanced self-evaluation include indoor hotspot (InH), urban microcell (UMi), urban macrocell (UMa), and rural macrocell (RMa). The network layout, carrier frequency, intersite distance, and UE speed of interest in these scenarios are shortlisted in Table 4.

The simulations are conducted using the same quasistatic system level simulator, according to guidelines for evaluation of radio interface technologies for IMT-Advanced [26] as well as additional modeling and assumptions for different ITU deployment scenarios [27]. ITU simulation methodology is slightly different from 3GPP counterpart mainly in

TABLE 4: ITU IMT-Advanced deployment scenarios.

| Test Environment     | Indoor         | Microcellular   | Base coverage urban | High speed      |
|----------------------|----------------|-----------------|---------------------|-----------------|
| Deployment scenario  | Indoor hotspot | Urban microcell | Urban macrocell     | Rural macrocell |
| Carrier frequency    | 3.4 GHz        | 2.5 GHz         | 2 GHz               | 800 MHz         |
| Layout               | Indoor floor   | Hexagonal grid  | Hexagonal grid      | Hexagonal grid  |
| Intersite distance   | 60 m           | 200 m           | 500 m               | 1732 m          |
| UE speed of interest | 3 km/h         | 3 km/h          | 30 km/h             | 120 km/h        |

TABLE 5: VoIP capacity requirement in IMT-Advanced and simulated results.

| Test scenario | Minimum required capacity<br>(Active users/sector/MHz) | Simulated capacity<br>(Active users/sector/MHz) |
|---------------|--|---|
| InH           | 50   | 105   |
| UMi           | 40   | 94  |
| UMa           | 40   | 80  |
| RMa           | 30   | 72  |

radio channel model and link budget setting. More details can be found in [26, 27]. Except that InH scenarios use a two-isolated cell layout, all the other three scenarios use the same simulated network layout as that used in 3GPP LTE simulations. VoIP traffic model, QoS criteria, link-to-system mapping model, and other simulation assumptions related to HARQ and CQI are the same as those used in the simulation of 3GPP LTE scenarios.

Table 5 summarizes the simulated VoIP capacity against IMT-Advanced requirements. Simulation results show enhanced VoIP capacity exceeds the requirements in all ITU test environments. It is concluded that IMT-Advanced requirements on VoIP capacity can be fulfilled with dynamic scheduling with proposed PDCCH resource allocation. Among these four scenarios, InH scenario includes only two-isolated cells with pedestrian users. UMi scenario has small intersite distance and includes pedestrian users only. Thus, high SINR and accurate CQI can be achieved in these two scenarios. PDCCH resource demand per user is not high and more users can be dynamically scheduled per TTI. In addition, frequency domain scheduling can be conducted efficiently and dynamic packet bundling can be utilized as much as possible. All these lead to high VoIP capacity. UMa scenario has slightly larger distance than that in InH and UMi scenarios and includes fast vehicular users. At speed of 30 km/h, the accuracy of CQI reported from UE begins to be vulnerable to fast changing radio channel conditions and gain from frequency domain scheduling and packet bundling might be reduced. On the other hand, due to relatively higher eNB transmission power in macro cell scenarios, the reserved higher PDCCH power leaves more room for efficient PDCCH power control and thus helps to boost VoIP capacity. RMa scenario has the largest intersite distance among all four scenarios and high-speed vehicular

users. The frequency domain scheduling gain is lost due to inaccurate CQI in fast changing radio channel condition. But PDCCH power can take advantage of relatively higher PDCCH power in macro cell scenario. In addition, PDCCH OLLA is capable of partly compensating for the CQI errors. All these help to sustain the capacity in lower SINR and control resource demanding situation.

## 6. Conclusions

In this paper, we studied PDCCH resource allocation method oriented for VoIP optimized dynamic scheduling. A comprehensive set of system level simulation results were demonstrated, covering both 3GPP LTE scenario and ITU IMT-Advanced scenario. A thorough analysis of capacity gain, PDCCH and PDSCH utilization rate, and packet delay performance were provided. Postsimulation analysis further confirms the effectiveness of proposed PDCCH resource allocation method. The proposed bidirectional power control algorithm can efficiently balance the allocation of CCE and power in PDCCH and maximize the number of users scheduled per TTI, thus greatly improving the capacity of VoIP with dynamic scheduling. The relative capacity gain is approximately 31–46% over that without power control, depending on deployment scenario and whether packet bundling is enabled or not. Besides, PDCCH resource allocation does not impose negative impact on packet bundling level and packet delay performance. Moreover, in all four ITU IMT-Advanced deployment scenarios, enhanced VoIP capacity exceeds the target set in IMT-Advanced. This approach can also be applied in semipersistent scheduling as the retransmissions and SID transmissions in semipersistent scheduling also needs control signaling. Although we use UTRAN LTE downlink as an application example in this paper, the proposed PDCCH resource allocation method can be naturally applied to UTRAN LTE uplink as well as other OFDMA-based mobile communication systems for VoIP performance enhancement.

## Acknowledgment

The authors appreciate the support from many colleagues, especially Markku Kuusela from Nokia Devices R&D, Helsinki and Petteri Lundén from Nokia Research Center, Helsinki in their study of VoIP on E-UTRA.

## References

- [1] H. Holma, M. Kuusela, E. Malkamäki, K. Ranto-aho, and T. Chen, "VoIP over HSPA with 3 GPP Release 7," in *Proceedings of IEEE International Symposium on Personal, Indoor and Mobile Radio Communications*, Helsinki, Finland, September 2006.
- [2] B. Wang, K. I. Pedersen, T. E. Kolding, and P. E. Mogensen, "Performance of VoIP on HSDPA," in *Proceedings of the 61st Vehicular Technology Conference (VTC '05)*, pp. 2335–2339, Stockholm, Sweden, June 2005.
- [3] P. Lundén and M. Kuusela, "Enhancing performance of VoIP over HSDPA," in *Proceedings of the 65th Vehicular Technology Conference (VTC '07)*, pp. 825–829, Dublin, Ireland, April 2007.
- [4] T. Chen, M. Kuusela, and E. Malkamäki, "Uplink capacity of VoIP on HSUPA," in *Proceedings of the 63rd Vehicular Technology Conference (VTC '06)*, pp. 451–455, Sydney, Australia, July 2006.
- [5] Third Generation Partnership Project, "Evolved Universal Terrestrial Radio Access (E-UTRA); Medium Access Control (MAC) protocol specification," TS 36.321, Release 8, 2008.
- [6] R. Love, R. Kuchibhotla, A. Ghosh et al., "Downlink control channel design for 3GPP LTE," in *Proceedings of IEEE Wireless Communications and Networking Conference (WCNC '08)*, pp. 813–818, Las Vegas, Nev, USA, April 2008.
- [7] R. Nory, R. Kuchibhotla, R. Love, S. Yakun, and X. Weimin, "Uplink VoIP support for 3GPP EUTRA," in *Proceedings of the 65th Vehicular Technology Conference (VTC '07)*, pp. 710–714, Dublin, Ireland, April 2007.
- [8] F. Persson, "Voice over IP realized for the 3GPP long term evolution," in *Proceedings of the 66th Vehicular Technology Conference (VTC '07)*, pp. 1436–1440, Baltimore, Md, USA, October 2007.
- [9] Y. Fan, M. Kuusela, P. Lundén, and M. Valkama, "Downlink VoIP support for Evolved UTRA," in *Proceedings of IEEE Wireless Communications and Networking Conference (WCNC '08)*, pp. 1933–1938, Las Vegas, Nev, USA, April 2008.
- [10] Y. Fan, P. Lundén, M. Kuusela, and M. Valkama, "Efficient semi-persistent scheduling for VoIP on EUTRA downlink," in *Proceedings of the 68th Semi-Annual IEEE Vehicular Technology Conference (VTC '08)*, Calgary, Canada, September 2008.
- [11] J. Puttonen, N. Kolehmainen, T. Henttonen, and M. Moision, "Persistent packet scheduling performance for voice-over-IP in evolved utran downlink," in *Proceedings of the 19th IEEE International Symposium on Personal, Indoor and Mobile Radio Communications (PIMRC '08)*, Cannes, France, September 2008.
- [12] M. Rinne, M. Kuusela, E. Tuomaala et al., "A performance summary of the evolved 3G (E-UTRA) for voice over internet and best effort traffic," *IEEE Transactions on Vehicular Technology*, vol. 58, no. 7, pp. 3661–3673, 2009.
- [13] J. Puttonen, H. H. Puupponen, K. Aho, T. Henttonen, and M. Moision, "Impact of control channel limitations on the LTE VoIP capacity," in *Proceedings of the 9th International Conference on Networks (ICN '10)*, pp. 77–82, Menuires, France, April 2010.
- [14] H. Holma, J. Kallio, M. Kuusela et al., "Voice over IP (VoIP)," in *LTE for UMTS: OFDMA and SC-FDMA Based Radio Access*, H. Holma and A. Toskala, Eds., chapter 10, pp. 259–281, John Wiley & Sons, New York, NY, USA, 2009.
- [15] D. López Villa, C. Úbeda Castellanos, I. Z. Kovács, F. Frederiksen, and K. I. Pedersen, "Performance of downlink UTRAN LTE under control channel constraints," in *Proceedings of the 67th Vehicular Technology Conference-Spring (VTC '08)*, pp. 2512–2516, Singapore, May 2008.
- [16] International Telecommunication Union, Rep. ITU-R M.2134, "Requirements related to technical performance for IMT-Advanced radio interface(s)," 2008.
- [17] Third Generation Partnership Project, "Physical Layer Aspects for evolved Universal Terrestrial Radio Access (UTRA)," TR 25.814, Release 7. version 7.1.0, September 2006.
- [18] International Telecommunication Union, "One way transmission time," Recommendation ITU-T G.114, February 2003.
- [19] Orange, China Mobile, KPN, NTT DoCoMo, Sprint, T-Mobile, Vodafone, Telecom Italia, "LTE physical layer framework for performance verification," R1-070674, 3GPP TSG-RAN1#48, St. Louis, Mich, February, 2007.
- [20] Y. Fan, P. Lundén, M. Kuusela, and M. Valkama, "Performance of VoIP on EUTRA downlink with limited channel feedback," in *Proceedings of IEEE International Symposium on Wireless Communication Systems (ISWCS '08)*, pp. 79–84, Rekjevik, Iceland, October 2008.
- [21] A. Sampath, P. S. Kumar, and J. M. Holtzman, "On setting reverse link target SIR in a CDMA system," in *Proceedings of the 1997 47th IEEE Vehicular Technology Conference. Part 1 (of 3)*, pp. 929–932, May 1997.
- [22] A. Jalali, R. Padovani, and R. Pankaj, "Data throughput of CDMA-HDR a high efficiency-high data rate personal communication wireless system," in *Proceedings of the 51st Vehicular Technology Conference (VTC '00)*, vol. 3, pp. 1854–1858, Tokyo, Japan, May 2000.
- [23] K. Brueninghaus, D. Astély, T. Sälzer et al., "Link performance models for system level simulations of broadband radio access systems," in *Proceedings of IEEE International Symposium on Personal, Indoor and Mobile Radio Communications (PIMRC '05)*, vol. 4, pp. 2306–2311, Berlin, Germany, September 2005.
- [24] Third Generation Partnership Project, "Mandatory speech CODEC speech processing functions; AMR speech Codec; General description," TS 26.071, July 2007.
- [25] Internet Engineering Task Force, "Robust Header Compression (ROHC)," IETF RFC 3095, July 2001.
- [26] International Telecommunication Union, "Guidelines for evaluation of radio interface technologies for IMT-Advanced," Rep. ITU-R M.2135, 2008.
- [27] Ericsson, "Radio characteristics of the ITU test environments and deployment scenarios," R1-091320, 3GPP TSG-RAN1#56bis, Seoul, Korea, March 2009.